搅拌针形状对搅拌摩擦焊焊缝截面形貌的影响

柯黎明[1,2]， 潘际銮[1]， 邢 丽[2]， 王善林[2]
（1. 清华大学 先进成形制造教育部重点实验室，北京 100084；
2. 南昌航空工业学院 材料科学与工程学院，南昌 330063）

柯黎明

摘 要：采用镶嵌异种材料作为标识材料的方法，用不同搅拌针形状的搅拌头，进行了搅拌摩擦焊试验。结果表明，搅拌针形状影响焊缝塑化金属流动的行为，导致焊缝截面形貌发生变化。搅拌针表面的反螺纹使搅拌针周围塑化金属向下流动，迫使搅拌针端部周边金属向上运动，焊核中心处于焊缝横截面下部；正螺纹使搅拌针周围塑化金属向上流动，迫使轴肩下方及周边金属向下运动，焊核中心处于焊缝横截面上部。改变搅拌针形状及长度，可以改变搅拌针下方及附近区域塑化金属的流动形态，从而改变焊缝底部的成形及包铝层进入焊缝的深度。

关键词：搅拌摩擦焊；搅拌针形状；塑性流动；焊缝形貌
中图分类号：TG453 文献标识码：A 文章编号：0253－360X(2007)05－033－05

0 序 言

搅拌摩擦焊(friction stir welding，简称 FSW)技术是英国焊接研究所(The Welding Institute，简称 TWI)1991 年发明的新型摩擦焊方法，自其发明以来，已得到全世界工业界的广泛关注。与传统的焊接方法相比，搅拌摩擦焊焊缝具有优异的力学性能，这一方法已成功地应用于航空、航天、汽车、船舶等领域。

目前，针对搅拌摩擦焊技术，各国研究者主要对有关铝合金搅拌摩擦焊的工艺、组织及力学性能进行了研究。Dawes[1] 和 Thomas[2] 分析总结了搅拌摩擦焊的基本焊接过程与特征；Liu[3]，Sutton[4] 和 Su 等人[5] 对 1000 系列、2000 系列、7000 系列的铝合金焊缝的组织、力学性能进行了研究；哈尔滨工业大学的王大勇等人[6] 提出了焊缝等轴再结晶晶粒的形成模型，分析了再结晶晶粒的形成原因；美国南卡罗来纳大学的 Deng[7] 和南昌航空工业学院的柯黎明等人[8] 用数值分析的方法分别建立了二维流动场模型，对焊缝塑化金属的流动行为进行了分析。

研究表明，除焊接速度、搅拌头旋转速度和搅拌头轴肩压力影响搅拌摩擦焊焊缝质量外，搅拌头形状对于搅拌摩擦焊焊缝的形成起着非常重要的作用。搅拌头形状参数主要包含三个方面：一是轴肩形状；二是搅拌针形状；三是搅拌针轴线与旋转中心的距离，即偏心距。TWI 开发了搅拌针形状为圆台形、带螺纹的圆锥形、偏心的圆柱形等多种形状的搅拌头，发现搅拌针形状变化会改变焊缝金属的受力状态，使焊缝金属的塑性流动性发生变化，进而影响焊缝的成形和力学性能[9]；Thomas[10] 设计了几种搅拌针形状为三槽形的搅拌头，发现这些搅拌头在搭接接头的焊接过程中能更好地破坏接头表面的氧化膜，促使焊缝金属充分流动，提高接头的力学性能。

文中用几种不同形状搅拌针的搅拌头，用镶嵌异种材料的方法，进行了搅拌摩擦焊试验，通过观察、分析试验结果，研究了搅拌针形状对搅拌摩擦焊焊缝塑化金属流动状态及焊缝截面形貌的影响。

1 试 验

采用 4 种不同形状搅拌针的搅拌头进行焊接试验，搅拌针的形状分别为：带反螺纹的圆柱形搅拌针，带正螺纹的圆柱形搅拌针，带反螺纹的圆锥形搅拌针，带反螺纹的凸轮形搅拌针。圆柱形搅拌针的直径为8 mm，长度为8 mm；圆锥形搅拌针的根部直径和端部直径分别为8 mm和4 mm，搅拌针长度为 8 mm。

试验用材料为板厚1 mm的 LY12、板厚2 mm的 LF6 铝合金，用厚0.02 mm的紫铜箔作为标识材料，交替叠放于铝合金薄板间。图 1 为标识材料的镶嵌

收稿日期：2006－06－07
基金项目：江西省自然科学基金资助项目(0450090)

方式，表层和底层材料为 LF6，中间交替叠放铜箔和 LY12，叠层总厚度为 8～9 mm。预先试验表明，厚度为0.02 mm的紫铜箔不会影响焊缝塑化金属的流动状态。在用铣床改装的搅拌摩擦焊设备上进行试验。焊接时，搅拌头顺时针旋转，焊接用的工艺参数：焊接速度为 60 mm/min，搅拌头的旋转速度为 750 r/min。焊后观察标识材料在焊缝横截面上的分布，分析焊缝金属在焊缝厚度方向的流动特征。

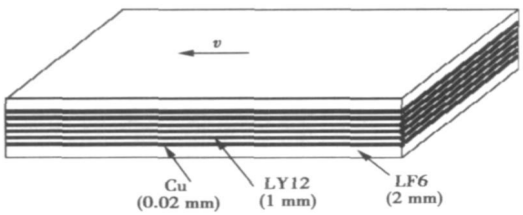

图 1 标识材料镶嵌方式示意图

Fig. 1 Schematics of inserted tracer material in samples

2 试验结果与讨论

2.1 试验结果

图 2 是用四种形状搅拌针的搅拌头焊接时得到的焊缝截面形貌，其中图 2a 为用带反螺纹圆柱形搅拌针的搅拌头焊接的焊缝横截面。可见，焊核呈明显的“洋葱瓣”花纹。“洋葱瓣”花纹的中心在焊缝的下方，标识材料在焊核中沿“洋葱瓣”花纹分布。在焊核区的外侧，标识材料的分布表明，塑化金属由焊缝底层向上流动。在返回边（retreating side，简称 RS），塑化金属流过焊核区上部，这种流动趋势一直延伸到前进边（advancing side，简称 AS）。在前进边，金属也向上流动，但仅分布在前进边一侧；在焊核区上部的标识材料呈平行焊缝表面分布。

图 2b 为用带正螺纹圆柱形搅拌针的搅拌头所焊接的焊缝横截面。由图可见，在焊核区也有“洋葱瓣”花纹形貌，但此时的“洋葱瓣”的中心位于焊缝的上方。由标识材料在焊缝横截面的分布表明，此时焊核区两侧的塑化金属呈向下流动的趋势，与图 2a 中塑化金属的流动方向相反。从两侧标识材料的分布看，前进边材料向下流动的趋势比返回边的大。在焊缝底部，金属的流动较图 2a 杂乱。返回边的金属向前进边流动，当流到焊缝中心时，与前进边的金属汇合形成紊流。紊乱区偏向前进边，而偏向返回边的近下表面，有部分与表面平行的层流区。

图 2c 和图 2d 分别是用带反螺纹的圆锥形和带反螺纹的凸轮形搅拌针焊接的焊缝横截面形貌。可见，这两种焊缝的焊核都位于焊缝截面的下方。在焊核区，标识材料呈弥散分布，没有明显的“洋葱瓣”花纹，焊核区两侧的塑化金属呈向上运动趋势，与图 2a 的相似。但是在图 2c 中，在前进边，标识材料向上弯曲的程度大于图 2a 中的相应位置，表明该处金属向上流动的趋势要大于图 2a 中的趋势。在返回边，塑化金属向上流至焊核区上部，一直延伸到前进边，且在焊核区的上部呈水平层流分布。在焊核区内，标识材料呈弥散分布，而且焊核区的形状不是上大下小的圆锥形，而是近似圆柱形。

图 2d 中标识材料在焊缝横截面上的分布表明，在前进边，金属向上流动的趋势较图 2a 和图 2c 的小，在返回边，塑化金属由底部向上流动，在焊核区上部，一直延伸到前进边侧，在焊核区上部，标识材料呈明显的水平层流分布，且层流区域比图 2a 和 2c 的大。

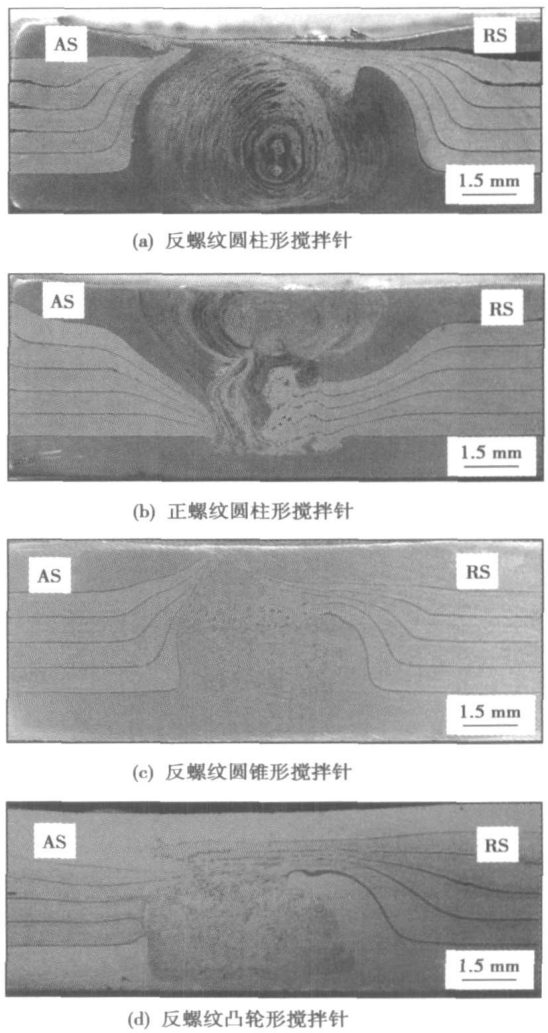

图 2 不同形状搅拌针焊接的焊缝截面形貌

Fig. 2 Morphology of weld transverse sections welded with different type of pins

上述结果表明，圆柱形带螺纹的搅拌针形成的焊缝截面形貌有明显的洋葱瓣特征，圆锥形搅拌针和凸轮形的搅拌针形成的焊缝截面上无洋葱瓣特征。搅拌针上螺纹的方向影响塑化金属的流动方向：反螺纹使洋葱瓣的中心向下移，正螺纹使洋葱瓣的中心向上移。搅拌针的形状影响塑化金属流动趋势大小，凸轮形搅拌针产生的流动趋势最大。

图 3 是用搅拌针尖端形状不同的搅拌头焊接时焊缝底部成形形貌，图中箭头所指为铝合金表面包铝层在焊缝内部的形态。当搅拌针尖端呈平面且离底面距离较小时，搅拌针正下方铝合金包铝层完全被挤向两侧并沿焊核边缘向上运动到接近板材中部，如图 3a 所示；当搅拌针尖端呈球面且离底面距离较大时，底表面包铝层沿焊核边缘向上运动的量较少，如图 3b 所示。而接头受拉时往往易于从焊核与包铝层的界面处断裂。

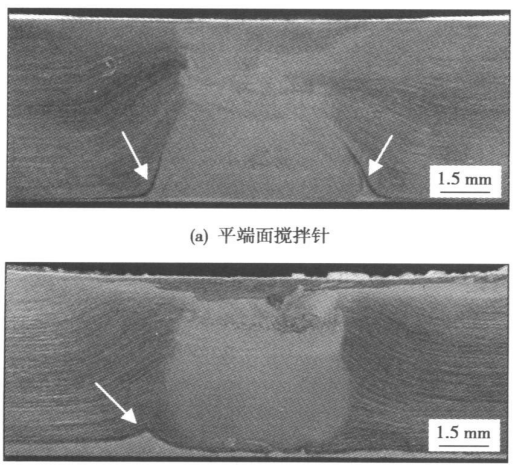

(a) 平端面搅拌针

(b) 球端面搅拌针

图 3　底表面包铝层沿焊核边缘向上运动的形貌

Fig. 3　Upward movement of aluminum layer on plate surface

2.2　试验结果分析

铝合金焊接时，焊缝温度一般为 450 ℃左右[10]，在此温度下，焊缝金属已呈粘塑性状态。焊接过程中，塑化金属并不是以相同速度随搅拌头一起运动，搅拌头与其周围塑化金属之间、塑化金属内不同的流动层之间存在速度差，因此在塑化金属与搅拌头、金属与金属之间存在摩擦[7]。搅拌头形状不同，与塑化金属之间的摩擦力方向各异，致使塑化金属的流动状态也不同。

搅拌头搅拌针上的螺纹方向不同，会对与之接触的塑化金属流动的驱动力不同。图 4 为当搅拌头沿 v 方向运动并以 w 速度作顺时针旋转时，焊缝金属受搅拌针螺纹作用力的示意图，图中 f_1，f_2 表示螺纹表面与塑化金属之间摩擦产生的摩擦力，p_1，p_2 为搅拌头旋转并向前运动时产生的垂直于螺纹表面的压力，n_1，n_2 分别为 p_1，f_1 和 p_2，f_2 的合力。图 4a 为用带反螺纹圆柱形搅拌针的搅拌头焊接时，搅拌针周围的塑化金属受到的作用力。在 p_1，f_1 两个力的作用下，塑性金属会产生两个方向的运动，一个是由摩擦力 f_1 作用产生的圆周运动，一个是压力 p_1 作用下的向下运动；两个力的综合作用，使搅拌针周围的塑化金属最终呈向下的螺旋形运动，其结果使搅拌针周围的塑化金属向下迁移；但在焊缝底层，塑化金属受底板的阻碍而向周边流动；从而在焊缝的上部出现瞬时的低压区或空腔，而在焊缝的下部局部区域形成较大的压力挤压焊核区外围的金属，导致外围金属受下部金属的高压区和上部金属低压区的压力差作用，向上运动。

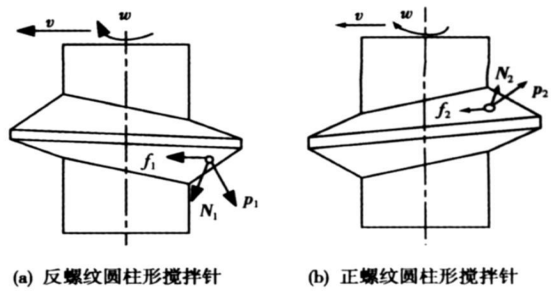

(a) 反螺纹圆柱形搅拌针　　(b) 正螺纹圆柱形搅拌针

图 4　焊缝金属受螺纹作用力的示意图

Fig. 4　Schematic drawings of interaction forces of plasticized metal around pin with screw thread in weld

带正螺纹圆柱形搅拌针的搅拌头对焊缝塑化金属的作用力与反螺纹的相反，如图 4b 所示。焊核区塑化金属在摩擦力 f_2 和压力 p_2 的共同作用下，向上作螺旋形运动，向上运动的塑化金属受轴肩挤压作用，随轴肩旋转并向外挤压，同时在搅拌针下部出现瞬时低压区。外围的塑化金属受轴肩处金属的挤压和焊缝下部出现的瞬时低压作用，呈向下运动。

图 5 为搅拌针表面为反螺纹的情况下，根据以上分析建立的焊缝塑化金属流动状态的物理模型示意图。此时，搅拌针周围塑化金属向下运动，在底部，由于受到底板的刚性阻碍，塑化金属朝周边运动并挤压周边金属，迫使搅拌针端部周边的金属朝上运动。在镶嵌有水平方向的标识材料的情况下，标识材料将向上弯曲，形成图 2a 中所见到的标识材料的分布状态。若焊缝上部瞬时空腔未被填充，就有可能在这个区域产生孔洞型缺陷，这与试验中观察到的缺陷分布位置一致。在搅拌针表面为正螺纹的

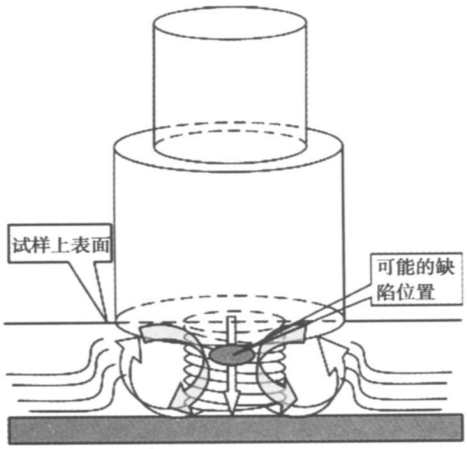

图 5 焊缝塑化金属流动状态的物理模型

Fig. 5 Physical model for flow state of plasticized metal in weld

情况下，流动状况与上述情形相反，水平方向的标识材料将向下弯曲，形成图 2b 中所见到的标识材料的分布状态，瞬时空腔位于搅拌针端部。试验发现，当用带正螺纹的搅拌头焊接厚板时，极易在焊缝下部形成缺陷。

搅拌头为带反螺纹的圆锥形和凸轮形搅拌针时，焊缝金属的受力状态与带反螺纹圆柱形搅拌针的周边金属的受力状态相似，因此，当搅拌头作顺时针方向旋转时，搅拌针表面的螺纹将驱动其周围金属向下运动。流动的塑化金属在底部受到刚性底板的阻碍作用，朝周边挤压原处于焊缝底部的金属，使其向更远的位置迁移，最后受到较远处温度较低的金属的阻碍而向上运动，形成一种塑化金属沿搅拌针周边向下运动、较远处金属向上运动的环形运动模式，最终形成图 2c 和图 2d 的形貌。但是，对于凸轮形搅拌针，旋转时其与周边塑化金属的接触状态不同于圆柱形搅拌针，尤其是其表面各点离等温面的距离在不断变化，使得搅拌针表面与周围较冷金属之间的塑化金属所受到的挤压作用也不断变化，最终形成比较紊乱的核心，焊核区标识材料呈弥散分布。

图 6 为搅拌针端部形状及其离板材底面的距离变化时搅拌针端部周围金属的流动状态示意图，点状区为铝合金表面的包铝层。当搅拌针尖端呈平面且离底面距离较小时，由螺纹驱动的塑化金属在搅拌针尖端脱离搅拌针并继续向下运动，将搅拌针下方的金属挤向周围区域，如图 6a 所示。不断向下运动的塑化金属沿底板表面朝周围运动，迫使这些区域原来的金属向离搅拌针尖端更远的区域运动，并在较远处冷金属的阻碍下朝上运动。这样，沿螺纹向下运动的塑化金属在焊缝底部形成一个焊核，原处于板材底面的包铝层也被运动的塑化金属带动并附在焊核外侧，随着塑化金属流的上升而进入焊缝内部，形成图 3a 所示的形态。当搅拌针尖端呈球面且离底面距离较大时，由螺纹驱动向下运动的塑化金属在离底面较远的位置离开搅拌针，然后继续向下及向周围运动，如图 6b 所示。此时，板材下表面的包铝层离搅拌针尖端较远，其连续性未被破坏，仅受到向下运动的塑化金属的压力作用及向周围运动的塑化金属的摩擦力作用，但这种摩擦力可能小于底板对包铝层的摩擦阻力。因此，包铝层位置不变或仅作少量的运动，如图 3b 所示。因此，改变搅拌针形状及长度，可以改变搅拌摩擦焊焊缝底部的成形。

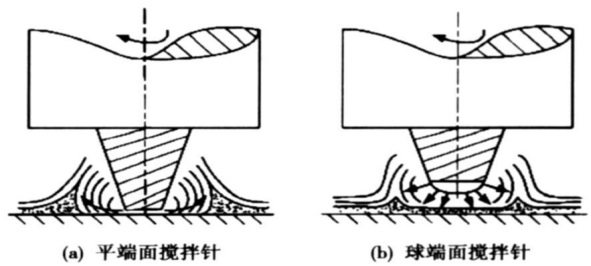

图 6 搅拌针端部形状对包铝层的影响

Fig. 6 Influence of tip shape of pin on aluminum layer on aluminum alloy

3 结 论

（1）搅拌针表面螺纹是驱动焊缝塑化金属沿板材厚度方向运动的主要因素，螺纹方向的变化会改变塑化金属的受力状态和流动形态，从而影响焊缝成形质量。反螺纹使搅拌针周围塑化金属向下流动，迫使搅拌针端部周边金属向上运动；正螺纹使搅拌针周围塑化金属向上流动，迫使轴肩下方及周边金属向下运动。在焊接工艺参数不合适的情况下，用反螺纹搅拌针焊接时易在焊缝上部出现缺陷，用正螺纹搅拌针焊接时易在焊缝下部出现缺陷。

（2）搅拌针形状会改变焊缝塑化金属所受到的挤压作用，从而改变金属的流动特征和迁移距离。圆柱形搅拌针形成的焊缝截面形貌有明显的洋葱瓣特征，圆锥形搅拌针和凸轮形的搅拌针形成的焊缝截面上无洋葱瓣特征；凸轮形搅拌针产生的迁移距离最大。

(3) 改变搅拌针形状及长度,可以改变搅拌针下方及附近区域塑化金属的流动形态,从而改变焊缝底部的成形及包铝层进入焊缝的深度。

参考文献:

[1] Dawes C J. An introduction to friction stir welding and its development[J]. Welding &Metal Fabrication, 1995, 74(1): 13—16.

[2] Thomas W M, Dolby R E. Friction stir welding developments[C] // Proceedings of the 6th international trends in welding research conference, Pine Mountain, Georgia(USA), 2002: 15—19.

[3] Liu Huijie. Heterogeneity of mechanical properties of friction stir welding joint of 1050—H24 aluminum alloy[J]. Journal of Materials Science Letters, 2003, 22(12): 441—444.

[4] Sutton M A, Yang B, Teynolds A P. Microstructure studies of fiction stir welds in 2024—T3 aluminum[J]. Materials Science and Engineering, 2002, A323(1—2): 160—166.

[5] Su J Q, Nelson T W, Mishra R. Microstructural investigation of friction stir welded 7050—T651 aluminum[J]. Acta Materialia, 2003, 51(3—7): 713—729.

[6] 王大勇,冯吉才. 铝合金搅拌摩擦焊接头焊核区等轴再结晶组织的形成机理[J]. 焊接学报, 2003, 23(4): 33—35.

[7] Deng Xiaomin, Xu Shapwen. Solid mechanics simulation of friction stir welding process[C] // Transactions of Namri/Sme, Gainesville, FL(USA), 2001, 29: 631—638.

[8] 柯黎明, 邢　丽, 黄奉安. 搅拌摩擦焊接头形成过程的二维观察与分析[J]. 焊接学报, 2005, 26(3): 1—4.

[9] Colegrove P A, Shercliff H R. Development of trivex friction stir welding tool Part 1-two-dimensional flow modelling and experimental validation[J]. Science and Technology of Welding and Joining, 2004, 9(4): 345—351.

[10] Thomas W M, Johnson K I, Wiesner C S. Friction stir welding-recent developments in tool and process technologies[J]. Advanced Engineering Materials, 2003, 5(7): 485—490.

作者简介:柯黎明,男,1960 年出生,教授,江西省中青年学科带头人。主要从事搅拌摩擦焊、扩散焊、钎焊、高温自蔓延合成焊接技术及其它先进焊接方法以及焊接过程的数值模拟。发表论文 40 余篇。

Email: liming_ke@126.com

Education, Lanzhou University of Technology, Lanzhou 730050, China; 2. State Key Laboratory of Advanced Non-ferrous Metal Materials, Lanzhou University of Technology, Lanzhou 730050, China). p17—20

Abstract: By using ANSYS, the 3D temperature field of laser welding for aluminum alloy of different thickness were simulated. In order to improve solution accuracy and efficiency, transition mesh and Gauss function heat source model were used, and APDL in ANSYS was used to compile program to realize the load of moving heat source. The effects of temperature-dependence material parameters and potential heat, boundary conditions, plasma, convection in molten pool and characteristics of different thickness were considered in the model. Using high-temperature thermocouple, the temperature was measured. It is shown that the simulation results are in accordance with the experimental results.

Key words: aluminum alloy; laser welding; different thickness; temperature field; numerical simulation

Effects of laser soldering speed on mechanical properties of SOP micro-joints XUE Songbai, HUANG Xiang, WU Yuxiu, HAN Zongjie (College of Materials Science and Technology, Nanjing University of Aeronautics and Astronautics, Nanjing 210016, China). p21—24

Abstract: SOP(small outline package) devices were soldered by diode-laser soldering and IR reflow soldering method respectively and the tensile strengths of soldered joints were measured by Micro-joints Tester(STR-1000), and the effects of laser soldering speed on mechanical properties of SOP micro-joints were studied and the characteristics of fracture microstructures of micro-joints were also analyzed by SEM. The results indicate that the tensile strength of soldered joints is influenced remarkably by laser soldering speed, and the mechanical properties of the joints soldered with Sn—Ag—Cu solder are more sensitive to soldering speed than that with Sn—Pb solder, and there is an optimal speed of laser soldering according to the best mechanical property. There are some micropores and shallow dimples when the speed is lower, which is called micropore aggregation fracture. There are plenty of dimples in the fracture and some sidesteps in the local zone of the fracture when the speed is higher, which the fracture includes dimple and cleavage fracture, and when the speed is moderate, there are lots of big and deep dimples in the fracture, which is the ductile fracture.

Key words: laser soldering; soldering speed; mechanical property

Brazing/hot-rolling technique for preparation of stainless steel/carbon steel cladding plate ZU Guoyin, YU Jiuming, WEN Jinglin (School of Materials and Metallurgy, Northeastern University, Shenyang 110004, China). p25—28

Abstract: Aiming at the main problems in the explosion-rolling bonding process of stainless steel/carbon steel cladding plate, a new technique of brazing/hot-rolling method was put forward, and the effect of main process parameter on the bonding strength of brazing cladding plate was studied, and the bonding mechanics of hot-rolling cladding plate was analyzed, and the main mechanical properties of cladding plate was tested. The results showed that an effective brazing bonding can be gotten by using home-made silver base solder. The oplimized processing parameters are as follows: brazing temperature is 755—770 ℃ and holding time is 2.5—3 min. Soldered layer shows good plasticity during hot-rolling process. When the deformation rate was 40%, there was no fracture and lamination in soldered layer after rolling. Metallic bonding formed between the soldered layer and the base metal, and the bonding strength of the stainless steel/soldered interface obviously increased, and the shear strength of cladding plate after hot-rolling can be reached 342.6 MPa.

Key words: stainless steel/carbon steel cladding plate; brazing; solder; hot-rolling; deformation rate

Effects of electrode pitting morphology on resistance spot welding of aluminum alloy CHANG Baohua[1], DU Dong[1], CHEN Qiang[1], Zhou Y[2]. (1. Department of Mechanical Engineering, Tsinghua University, Beijing 100084, China; 2. Department of Mechanical Engineering, University of Waterloo, Waterloo, Ontario, N2L 3G1, Canada). p29—32

Abstract: The effects of two types of electrode pitting morphologies, ring type and hole type on resistance spot welding of aluminum alloy 5182 were investigated by the combination of finite element analysis and physical modeling methods. Results showed that when using ring pitting electrode, the contact radius at faying surface is increased while the current distribution is not affected notably, and the nugget diameter is increased. When using hole pitting electrode, the contact radius at faying surface is increased further and the current density is decreased in the contact region. In addition, electric current does not flows through the central part of faying surface under such conditions, consequently, central part does not melt and only donut shape nugget is formed. Hole type pitting reduces the joint strength significantly, and its detrimental influence on joint quality is much greater than that of ring type pitting.

Key words: resistance spot welding; pitting; electrode degradation; aluminum alloys; finite element method

Influence of pin shape on weld transverse morphology in friction stir welding KE Liming[1,2], PAN Jiluan[1], XING Li[2], WANG Shanlin[2](1. Key Laboratory for Advanced Manufacturing by Materials Processing Technology, The Ministry of Education, Tsinghua University, Beijing 100084, China; 2. Department of Materials Science and Engineering, Nanchang Institute of Aero-Technology, Nanchang 330063, China). p33—37

Abstract: Friction stir welding was conducted by using four types of pin and copper foils, piled up with aluminum plate alternately, as a tracer material. The distribution feature of the tracer materials was observed after welding. The results showed that, the flow of the plasticized metal in the weld is influenced by the pin shopes, which results in the variety of the morphology of the weld. If the screw thread on the pin is counter-clockwise, the metal around the pin will move downwards, which drives the metal around the pin tip to move around and upwards. So the center of the nugget is located at the lower part of the tansverse weld section. If the screw thread

on the pin is clockwise, the metal around the pin will move upwards to the root of the pin and moves outwards along the shoulder surface, which causes that the center of the nugget will located at the upper part of the weld section. By using the pin with cylindrical shape, the transverse weld section appears onion ring pattern; but the onion ring pattern is not clear in the weld transverse section for the pin with taper shape or cam shape. If the length of the pin and shape at the tip are changed, the flow state of the plasticized metal below the pin and around the tip of the pin will be changed, therefore, the morphology of the weld at the bottom will change and the depth that the aluminum layer on the back surface of the plate enteed into the weld will be larger.

Key words: friction stir welding; pin shape; plastic flow; transverse weld morphology

Extraction of diagnostic information of expulsion defect in resistance spot welding process by wavelet analysis method XUE Haitao, LI Yongyan, CUI Chunxiang, DONG Tianshun (School of Material Science and Engineering, Hebei University of Technology, Tianjin 300132, China). p38—40

Abstract: An effective approach was developed to extract diagnostic information used to identify expulsion from electrode force curve by using wavelets analysis method for aluminum alloy shock wave resistance spot welding. The irregular signal singularity of electrode force curve was detected by using db5 wavelet. The detection result shows that the location and intensity of the signal singularity can be detected accurately from high frequency reconstructed signal of wavelet decomposition structure. That is to say, the expulsion can be identified easily. The diagnostic information is the global maximum value of high frequency reconstructed signal. The recognition method is that if the global maximum value exceeds the threshold value built by analyzing a number of testing data, the expulsion will occur. The testing result proves that the method is correct, reliable and credible. Therefore, the signal characteristic of electrode fore curve can be transformed into numerical characteristic that can be identified by computer.

Key words: aluminum alloy resistance spot welding; expulsion; wavelet analysis; diagnostic information

Effect of TiB_2 on microstructure and properties of Ni-based alloy coating by laser cladding YUAN Xiaomin, GONG Youpin, HE Yizhu (Anhui Key Laboratory of Materials and Processing, Anhui University of Technology, Maanshan 243002, Anhui, China). p41—44

Abstract: Ni-base alloy and TiB_2/Ni-based alloy metal-ceramics coatings were obtained on low carbon steel surface by 5 kW CO_2 laser. Microstructure, phases, microhardness and sliding wear resistance of the coatings were studied. The results shown that Ni-based alloy coating consists of γ-(Ni, Fe), $Cr_{23}C_6$ etc and TiB_2/Ni-based alloy composite coating consists of γ-(Ni, Fe), Ni_3B, TiB_2 and TiC and so on. The Ni-based alloy coating is made up of flourishing γ-(Ni, Fe) dendrite and eutectic structure. Equiaxed solid solution and fine eutectic structure are observed in the TiB_2/Ni-based alloy composite coating. The influence of TiB_2 ceramics on microstructure of coating is prominent that the microstructure of coating is finer and the dendrite crystal gradually becomes equiaxed grain. The microhardness and wear resistance of Ni-based alloy can be improved remarkablely by adding TiB_2.

Key words: laser cladding; Ni-based alloy; TiB_2; metal-ceramics layers; microstructure

Effect of magetic field parameters on microstructure and properties of welded joint of AZ31 magnesium alloy SU Yunhai[1], LIU Zhengjun[1], WANG Yu[2], ZHANG Guiqing[1] (1. Department of Material Sciences and Engineering, Shenyang University of Technology, Shenyang 110023, China; 2. Shenyang Special Type Equipment Examining Academe, Shenyang 110035, China). p45—48

Abstract: AC lognitudinal magnetic field was employed in welding of 5 mm thick AZ31 magnesium alloy plate with GTAW. The effect of magnetic field parameters on properties and microstructure of welded joint of AZ31 was studied through analysing the tensile strength, hardness and microstruture. The action mechanism of magnetic field was explored. The results indicated that the molten pool is stirred by the AC lognitudinal magnetic field, the solidification process is changed, the crystal grain is refined, and tensile strength and hardness of welded joint are improved. The molten pool is purified by the eletromagnetic stirring, so the gas pore and sensitivity of hot crack are decreased, and the formation of hot crack was supressed.

Key words: alternating current longitudinal magnetic field; AZ31magnesium alloy; gas tungsten arc welding; mechanical property

Numerical simulation of temperature field on complicated parts during plasma deposition dieless manufacturing WANG Guilan[1], WU Shengchuan[2], ZHANG Haiou[2] (1. College of Material Science and Engineering, Huazhong University of Science and Technology, Wuhan 430074, China; 2. State Key Laboratory of Digital Manufacturing Equipment and Technology, Huazhong University of Science and Technology, Wuhan 430074, China). p49—52

Abstract: A hybrid Gauss-double-Ellipse heat source model and a radiation-convection model were introduced to simulate plasma arc heat source and thermal boundary conditions. To improve the computational efficiency and reproduce the forming process, element Death & Birth and adaptive mesh techniques were used especially. Moreover, APDL code was developed to optimize fabrication process of a complicated part by plasma deposition dieless manufacturing, and some experiments were also conducted. Numerical and experimental results show that symmetrical jump-scanned paths together with suitable heat input and cooling approaches are effectively to improve the temperature distribution of parts and free contractility of weld, and thus lower stress level and hot crackability can be obtained, which eventually improve the possibly-intended formability.

Key words: plasma deposition dieless manufacturing; temperature field; finite element analysis; symmetrical jump-scanned paths; hot crackability

Transient liquid phase bonding of 45MnMoB steel geological